Journal of Applied Polymer Science

# Enhancement of Fibroblastic Proliferation from Photoreactive Starch with Immobilized Epidermal Growth Factor

**Young-Min Cho, Hyung-Jae Lee, Yun Heo, Shin-Hye Park, Si-Yoong Seo, Jae-Hong Han, Tae-Il Son**
Department of Biotechnology and Bio-Environmental Technology (BET) Research Institute, Chung-Ang University, Anseong, Gyeonggi-do 456-756, South Korea
Correspondence to: T.-I. Son (E-mail: tisohn@cau.ac.kr)

**ABSTRACT:** Carboxymethyl starch was modified by the incorporation of an azidophenyl group to prepare photoreactive starch, and characterized by Fourier transform infrared reflectance (FT-IR), proton nuclear magnetic resonance ($^1$H-NMR), and ultraviolet (UV) spectroscopy. Photo-irradiation immobilized the Az-starch on a polystyrene plate and it was stably retained on the surface. The protein containing immobilized Az-starch was also immobilized on a stripe micropatterned plate. UV irradiation time and Az-starch concentration were used to alter the physical properties of Az-starch and consequently control the rate of epidermal growth factor (EGF) release. The Az-starch that released growth factor was not cytotoxic to 3T3-L1 fibroblast cells, and the immobilized EGF maintained its activity and induced cellular proliferation *in vitro*. These results suggest that Az-starch could be useful as a clinical synthetic material for medical applications. © 2013 Wiley Periodicals, Inc. J. Appl. Polym. Sci. 129: 2161–2170, 2013

**KEYWORDS:** bioengineering; biomaterials; biomedical applications; drug delivery systems; photopolymerization

Received 5 August 2012; accepted 7 December 2012; published online 15 January 2013
**DOI: 10.1002/app.38919**

## INTRODUCTION

Growth factors are proteins that play an important role in the modulation of tissue growth and development, and therefore are considered essential elements in a variety of tissue engineering strategies.[1,2] It was reported that growth factors, as high molecular weight bio-signals, interact with related cell surface receptors to form a complex in the soluble state, which then aggregates on the cell surface before being internalized into the cell. The internalized complex is dissociated and decomposed in lysosomes.[3] The continuous effect of growth factors on mitogenic activity is decreased as a result of this rapid internalization process.

The immobilization of growth factors on various biomaterial matrices has been addressed by many studies examining the release of slowly diffusible growth factors for continuous delivery to sites of tissue target. Such biomaterial immobilization systems are often ineffective and costly due to unpredictable release characteristics from the matrices or needs of large amounts of soluble growth factors to effect cellular interaction with its cognate receptors.[4] Specifically, when large amounts of growth factors are immobilized on a matrix, uncontrolled large quantities of epidermal growth factor (EGF) have potential to damage cells and tissues.[5,6]

Water-soluble carbodiimide (WSC) chemistry has typically been used for immobilization of growth factors by 1-ethyl-3-(3-dimethylaminopropyl)carbodiimide (EDC). However, the *o*-acylisourea intermediate formed in the EDC reaction is highly unstable in aqueous solution and susceptible to hydrolysis, which results in reformation of the carboxylic acid. Moreover, the EDC is capable of not only binding growth factor to substrate, but can also crosslink the substrate to itself, although the addition of *N*-hydroxysuccinimide (NHS) improves the efficiency of EDC-mediated coupling reactions.[7]

For the reasons noted above, the photo-immobilization method recently has been increasingly studied in biomedical applications. In addition, this process can be carried out on any organic material, including biological molecules and polymer matrices by radical cross-reactions, which do not require any special functional groups unlike the WSC chemistry method.[8] As a light source induces the reactions, the delivery of immobilized growth factors can be controlled by manipulating the light exposure of a substrate.[9] In addition, this method is mild, biomolecule friendly and independent of pH and temperature.

Many different reactive groups have been introduced to substrates for immobilization of bioactive molecules such as growth factors onto matrices by the photo-immobilization methods.[10,11] Of these groups, phenyl azides as photoreactive cross-linker generally have the property of a lower energy of activation and hydroxyl groups on their aromatic ring, which allows activation close to 350 nm wavelength ultraviolet (UV) light and short

irradiation time. Minimizing irradiation time and using long-wavelength UV light decreases the risk of altering growth factor activity or cell viability.[12]

A variety of biomaterials have been employed as substrate in previous studies. Relatively few studies have used starch-based polymer as a component for these types of applications, despite it being well known that they are biocompatible, nontoxic and biodegradable materials. The versatility of the applications available for this substrate is unparalleled as compared with other biomaterials. Starch is generally a nonpolluting renewable source for a sustainable supply of cheaper pharmaceutical products. It is a major component of dusting powder, pastes and ointments meant to provide protective and healing effects on skin. Recently, starch-based polymers, in the form of microspheres or hydrogel, have been utilized in controlled-release biomaterials for the delivery of drugs such as hormones.[13,14]

In this study, we applied the photo-immobilization method to immobilize growth factor in starch matrix by inducing radical reactions with phenyl azide. FT-IR, $^1$H-NMR and UV spectroscopy were used to characterize the structure of the modified starch. All cell culture studies and cytotoxicity assays were performed with the 3T3-L1 cell line. The effect of immobilized growth factor on cell growth was investigated using 3-(4,5-dimethylthiazol-2-yl)-diphenyltetrazolium bromide (MTT) assays. *In vitro* protein release was assessed using bovine serum albumin (BSA).

## EXPERIMENTAL

### Materials

For the synthesis of photoreactive starch, wheat starch, *N*-(3-Dimethylaminopropyl)-*N′*-ethylcarbodiimide hydrochloride (EDC) and 4-azidoaniline hydrochloride was purchased from Sigma-Aldrich (St. Louis, MO). Sodium hydroxide was purchased from Duksan Pure Chemical Co. Ltd (Ansan, Korea). Monochloroacetic acid was purchased from Tokyo Chemical Industry (Tokyo, Japan). Hydrochloric acid, acetone, ether, ethanol, acetic acid and isopropanol were purchased from Samchun Pure Chemical (Seoul, Korea). The chemicals were used as received. For the cell cultures and the protein immobilization, Dulbecco's phosphate buffered saline (D-PBS) and Dulbecco's modified Eagle's medium (DMEM) (high glucose) with L-glutamine and phenol red was purchased from Wako Pure Chemical Ind. (Osaka, Japan). fetal bovine serum (FBS) was purchased from Gibco® (Eggenstein, Germany). Trypsin-EDTA solution (1×), BSA and fluorescein isothiocynate conjugated BSA (FITC-BSA) was purchased from Sigma-Aldrich Co. (St. Louis, MO). EGF was purchased from ProSpec-Tany Technogene Ltd. (Rehovot, Israel).

### Preparation of Carboxymethyl Starch

Modification of the carboxymethyl starch was performed as follows. Wheat starch (1.8 g, 0.01 mol) was suspended in 60 mL 1 *N* HCl and was stirred vigorously for 24 h at 60°C. The reaction mixture was neutralized with 1% (w/v) aqueous solution of sodium hydroxide. The mixture was dialyzed using a seamless cellulose dialysis tube with a 12,000 MW cut-off (Cellu•Sep T4, Membrane Filtration Products, Seguin, TX) in double distilled water for 3 days. The dialyzed solution was filtered and then vacuum-dried at room temperature.

The carboxymethyl starch was prepared by a variant of a previously reported method for carboxymethylation developed by Volkert et al.[15] Mono-chloroacetic acid (9.45 g, 0.1 mol) was dissolved in 300 mL isopropanol and neutralized with 45% (v/v) aqueous solution of sodium hydroxide (8.89 g). Acid-treated starch (4.5 g, 0.025 mol) and NaOH (2.4 g) were subsequently added to the mixture under vigorous stirring. The reaction mixture was left to stand for 5 h at 40°C and was subsequently neutralized with aqueous acetic acid. The starch was repeatedly washed with an excess of 80% aqueous methanol solution, which was evaporated under reduced pressure. The mixture was then dissolved in double distilled water and dialyzed using a seamless cellulose dialysis tube with a 12,000 MW cut-off in double distilled water for 3 days. The dialyzed solution was filtered and then lyophilized using a freeze-dryer (FDU-2200, Eyela, Tokyo, Japan) under reduced pressure.

### Synthesis of Photoreactive Polymers

The azido-modified starch was synthesized as previously reported.[16] In brief, carboxymethyl starch (1 g) was dissolved in 100 mL of aqueous sodium hydroxide (0.1 *N*). The starch solution was neutralized to pH 7.5 with 1.0 *N* hydrochloric acid. After EDC was dissolved in PBS (45 mL), the solution was added to the reaction mixture under stirring at 4°C, and 4-azidoanilne (88 mg) was subsequently added. The reaction mixture was stirred for two days at 4°C, and then stirred for two days at room temperature in the dark. Then, the reaction mixture was evaporated under reduced pressure, dissolved in double distilled water and dialyzed using a seamless cellulose dialysis tube with a 12,000 MW cut-off for 3 days. The dialyzed solution was filtered, and then lyophilized using a freeze-dryer under reduced pressure. The photoreactive starch is referred to as Az-starch hereafter. The synthetic scheme of Az-starch is shown in Figure 1(a).

### Spectroscopic Measurements of the Photoreactive Polymer

Acid-treated starch, carboxymethyl starch and Az-starch were measured with a FT-IR spectrometer (FT-IR 8400S, Shimadzu, Kyoto, Japan) at room temperature. The dried samples were triturated with a KBr ratio of 1 : 100 and pellets were prepared using a hydraulic compression instrument (SSP-10A, Shimadzu, Kyoto, Japan). The spectra of all samples were scanned from 400 to 4000 $cm^{-1}$ in transmission mode.

To further confirm the structure and properties of Az-starch, the UV spectra of Az-starch, 4-azidoaniline and carboxymethyl starch were measured with a UV/VIS spectrophotometer (T-60, Eyela, Tokyo, Japan). The samples dissolved in double distilled water were placed in a rectangular 1 cm quartz cell, and UV spectra of the sample solutions were recorded from 230 to 310 nm. The $^1$H-NMR spectra of carboxymethyl starch and Az-starch were measured with a 600 MHz NMR spectrometer (VNS, Varian Inc., Palo Alto, CA) in $D_2O$ at a concentration of 50 mg/mL.

### Photo-curing Characteristics

The photo-reactive Az-starch was dissolved in double distilled water at various concentrations. Aqueous solutions of Az-starch were cast on polystyrene plates and air-dried for 24 h at room

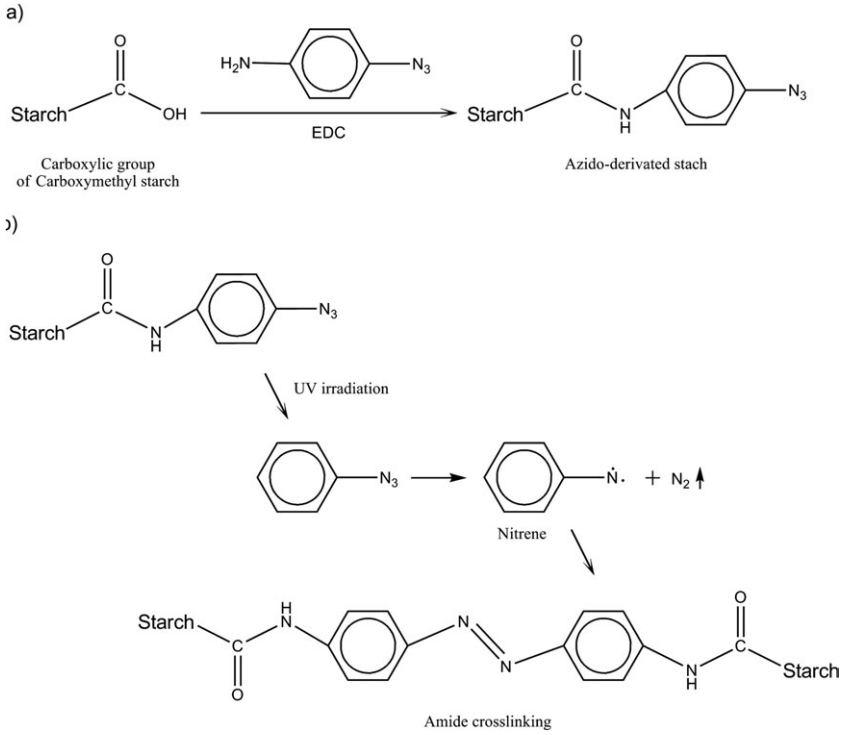


**Figure 1.** Scheme of (a) chemical reaction process for Az-starch and (b) production of nitrene groups in Az-starch by UV irradiation.

temperature. Dried sample plates were weighed and then irradiated with UV light by varying the irradiation time. The samples were then immersed in 5 mL of distilled water for 2 h at 37°C to remove the unreacted Az-starch. The purified samples were dried for 24 h at 37°C and then weighed. This experiment was performed three times for each sample and the yield was calculated using the following equation:

$$\text{Gel yield } (\%) = W_{\text{gel}}/W_{\text{solid}} \times 100$$

($W_{\text{Gel}}$ and $W_{\text{Solid}}$ are the weight of dry gel and the weight of dry gel after washing, respectively).

### Micropattern Immobilization

Aqueous solutions of Az-starch with/without the FITC-BSA (10 mg/mL) were cast on 24-well tissue culture polystyrene plates (Jet Bio-filtration Products, Guangzhou, China) and air-dried at room temperature in the dark. The cast surfaces were irradiated with Spot UV curing equipment (Spot Cure SP-9, Ushio Tokyo, Japan), equipped with a deep UV lamp (200 W) for 30 s from 5 cm above the surface of the stripe micropatterned plate (Nepco, Ansan, Korea). After removing the stripe micropatterned plate, the irradiated surfaces were then washed three times with double distilled water to remove nonirradiated Az-modified starch. The micropatterned surfaces were observed using optical microscopy (CBS-IH5, Samwon scientific Ind., Seoul, Korea) and fluorescence microscopy (Eclipse TE2000-U, Nikon Sankei, Tokyo, Japan), respectively. The surface properties of the photo-immobilized Az-starch were measured with an automatic contact angle meter (CA-W, Kyowa interface Science, Saitama, Japan) at room temperature with 0.4 $\mu$L distilled water droplets. Droplets of water were applied to different areas to calculate the average contact angle for the sample surface.

### Cytotoxicity Assay

Cytotoxicity was assessed using the WST-8 assay with a cell counting kit-8 (CCK-8; Dojindo Laboratories, Kumamoto, Japan). 3T3-L1 cells (fibroblast cells originating from a Swiss albino mouse embryo) were obtained from the Korean Cell Line Bank (Seoul, Korea) and were subcultured in DMEM with L-glutamine and phenol red supplemented with 10% (v/v) FBS at 37°C in a 5% (v/v) $CO_2$ atmosphere (Vision Scientific, Korea). After each well was checked for cell attachment, the media was removed and replaced with fresh media containing 5% (v/v) FBS. Aqueous sample solutions were added to each well of a 96-well tissue culture plate at concentrations of 1, 3, and 5%. After incubation for 12–48 h, the mixed media was removed and replaced with 50 $\mu$L of culture media with 10% (v/v) WST-8 solution per well. Samples were then incubated for an additional 1 h at 37°C in a 5% (v/v) $CO_2$ atmosphere. The absorbance of the water-soluble formazan produced from each well was measured at 450 nm with a microplate reader (Spectramax 190, Molecular Devices, CA). The cell viability was calculated using the following equation:

$$\text{Cell viability } (\%) = (\text{OD}_{450(\text{sample})}/\text{OD}_{450(\text{control})}) \times 100,$$

where $\text{OD}_{450(\text{sample})}$ is the absorbance of the culture medium with sample solutions and $\text{OD}_{450(\text{control})}$ is the absorbance at 450 nm of the negative control containing culture medium without sample solutions.

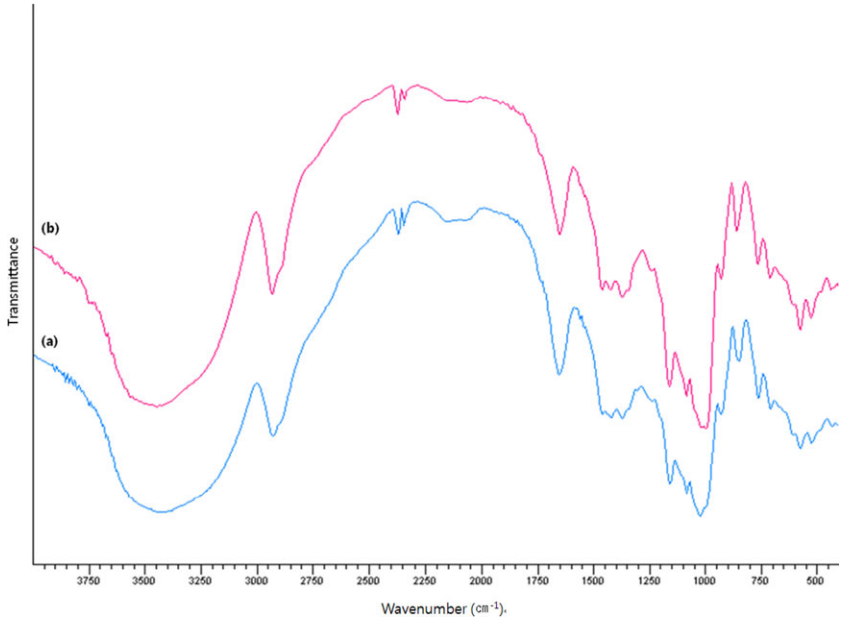


**Figure 2.** FT-IR spectra of (a) acid-treated starch and (b) native starch. [Color figure can be viewed in the online issue, which is available at wileyonlinelibrary.com.]

### Cell Culture

3T3-L1 cells were subcultured in DMEM with L-glutamine and phenol red supplemented with 10% (v/v) FBS at 37°C in a 5% (v/v) $CO_2$ atmosphere. The cultured cells were harvested with 1× trypsin-EDTA solution. After washing with culture medium, the cells were resuspended in fresh medium ($2.0 \times 10^4$ cell/mL). The cell suspensions were added to a 12-well sample plate, which had been sterilized with 70% ethanol, and then cultured at 37°C in a 5% (v/v) $CO_2$ atmosphere. After incubation for 24 h, the cells were washed twice with D-PBS to remove unattached cells. Cell morphology was observed by optical microscopy.

### *In Vitro* Protein Release

Aqueous solutions of sample containing BSA solution were cast on polystyrene plates and exposed to UV light for predetermined times. The immobilized samples were then incubated in 1 mL release medium at room temperature. The supernatant was withdrawn at regular intervals and replaced with 1 mL of fresh release medium (PBS buffer, pH 7.4) to maintain the total incubation volume. The amount of BSA released from the immobilized samples was determined by measuring aliquots in the supernatant and detected via the Coomassie Brilliant Blue (CBB) method at 595 nm using a UV/VIS spectrophotometer. All measurements were performed in triplicate and the cumulative protein release was calculated. Blank samples without protein were also analyzed according to the same procedure. No absorption bands were seen in the blank samples, which demonstrated that the degradation products did not interfere with the CBB experiment.[17]

### Cell Growth Assay on an EGF-immobilized Surface

Aqueous solutions of Az-starch containing EGF solution (50 μg/mL) were cast in 24-well tissue culture plates and air-dried at room temperature in the dark. The cast surfaces were irradiated with UV light for 90 s from 5 cm above the surface. 3T3-L1 cells were subcultured in DMEM with L-glutamine and phenol red supplemented with 10% (v/v) FBS at 37°C in a 5% (v/v) $CO_2$ atmosphere. After incubation for 24 h, the culture medium was replaced with fresh DMEM. The cells were plated at a density of $2.0 \times 10^4$ cells/mL in each well of the culture plate and incubated at 37°C in a 5(v/v) % $CO_2$ atmosphere for 4 days. Cell growth was estimated by the amount of formazan uptake. After incubation for 24, 48, 72 and 96 h, the cells were incubated for an additional 4 h at 37°C in the presence of MTT solution. Thereafter, the MTT solution was removed and DMSO solution was added to dissolve the formazan crystals. The absorbance of the water-soluble formazan produced from each well was measured at 595 nm with a UV/VIS spectrophotometer.

## RESULTS AND DISCUSSION

### Spectroscopic Analyses

The FT-IR spectra of native and acid-treated starch samples are shown in Figure 2. In the fingerprint region of the spectrum of native starch, there were several characteristic peaks between 900 and 1200 $cm^{-1}$. These peaks are due to C—O bond stretching.[18] The peaks observed at 1023 and 1083 $cm^{-1}$ are due to C—O stretching in the anhydroglucose ring. The characteristic peak at 1640 $cm^{-1}$ is associated with tightly bound water present in starch.[19,20] An extremely broad and intense peak at 3455 $cm^{-1}$ attributed to the complex stretching vibrations is associated with the free intra- and intermolecularly bound —OH groups that form the structure of native starch. The sharp peak at 2933 $cm^{-1}$ was assigned to C—H stretching associated with ring methine hydrogen atoms.[21] In contrast, acid-treatment of starch was found to cause an increase in the peak intensity at 1019 $cm^{-1}$. The broadening of the peak interfered with the

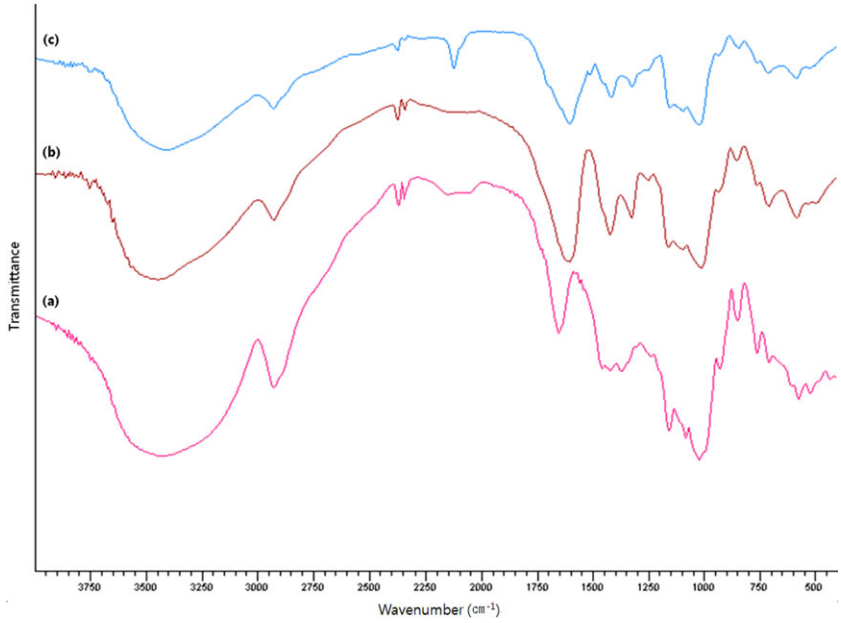


**Figure 3.** FT-IR spectra of (a) acid-treated starch, (b) carboxymethyl starch and (c) Az-starch. [Color figure can be viewed in the online issue, which is available at wileyonlinelibrary.com.]

decreasing intensity of the band at 995 $cm^{-1}$. The changes in peak intensities were attributed to the change in specific starch conformations, such as long-range ordering and crystallinity, as suggested by van Soeat et al.[22]

FT-IR spectra of carboxymethyl starch and Az-starch are shown in Figure 3. Characteristic of the native starch moiety, the spectrum of carboxymethyl starch showed intense peaks at 1023, 1083 and 1158 $cm^{-1}$. The peaks observed at 764, 860 and 927 $cm^{-1}$ were associated with α-configuration of the glycosidic linkage for starch. The characteristic peaks observed at 1605 and 1422 $cm^{-1}$ originated from resonances of the carboxylic groups of carboxymethyl substituents.[23] The Az-starch spectrum comprised two characteristic peaks at 1510 and 2120 $cm^{-1}$ when compared with the spectrum of carboxymethyl starch. These peaks are associated with the fact that the carboxylic groups of carboxymethyl starch were involved in the covalent bonding with amino groups of 4-azidoaniline. The peaks observed at 1510 and 2120 $cm^{-1}$ corresponded to N—H bending (amide II) and the azido group, respectively.[24]

UV spectra of Az-starch, 4-azidoanilne and carboxymethyl starch are shown in Figure 4. The wavelengths of maximum absorption ($\lambda_{max}$) for Az-starch and 4-azidoanilne were recorded at 267 and 257 nm, respectively. However, the UV spectra of carboxymethyl starch did not show the characteristic absorptions of polysaccharides at 230–310 nm. The broad band for 4-azidoaniline was assigned to the azidophenyl group, and it was shifted to a lower wavelength for Az-starch. The shift of the absorption band for the Az-starch could be due to the fact that the carboxyl groups (COO—) of carboxymethyl starch are partially involved in covalent bonding with the amino groups (—$NH_2$) of 4-azidoaniline. According to the previously reported method, the molecular absorption coefficient of the azidophenyl group at 257 nm can be calculated by comparison with that of 4-azidoaniline at 267 nm. The azidophenyl group content in Az-starch was about 0.02 mol/mol monosaccharide unit.[16]

Az-starch and carboxymethyl starch were measured with a 600 MHz $^1$H-NMR spectrometer. The characteristic spectrum of Az-starch is shown in Figure 5. The peaks observed at 7.08 and 7.43 ppm were assigned to protons on the phenyl ring in Az-starch. This indicates that the amino groups of 4-azidoanilne were successfully conjugated to the carboxyl groups of carboxymethyl starch. The degree of substitution (DS) for the

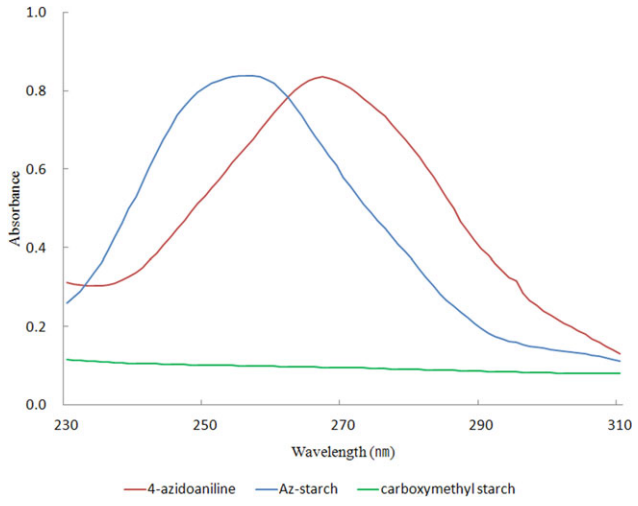


**Figure 4.** UV absorption spectra of (a) 4-azidoanilne (7.81 μg/mL), (b) Az-starch (125 μg/mL) and (c) carboxymethyl starch (125 μg/mL). The wavelengths of maximum absorption ($\lambda_{max}$) for Az-starch and 4-azidoaniline were recorded at 267 and 257 nm, respectively. [Color figure can be viewed in the online issue, which is available at wileyonlinelibrary.com.]

Applied Polymer SCIENCE

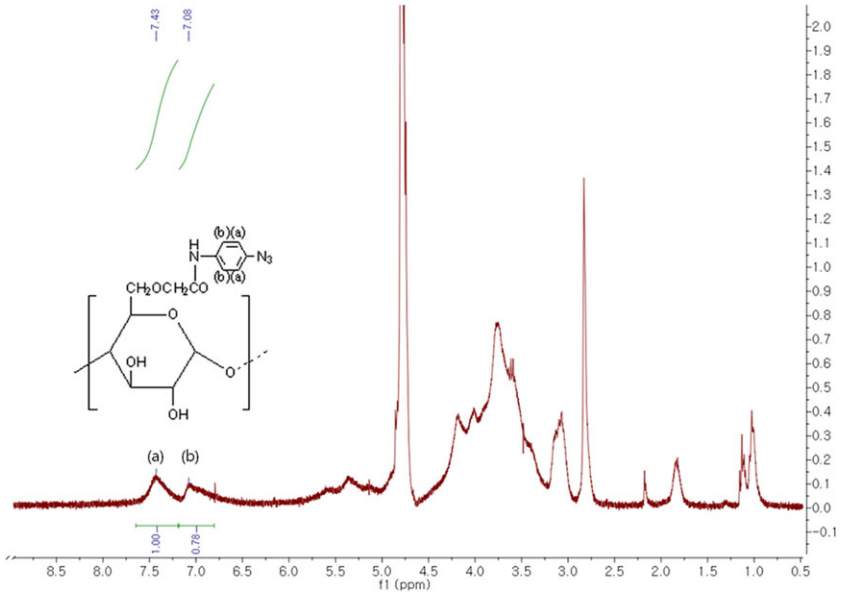


**Figure 5.** [1]H-NMR spectra of Az-starch. Characteristic peaks of aromatic protons in azidophenyl groups were observed at 7.08 and 7.43 ppm. [Color figure can be viewed in the online issue, which is available at wileyonlinelibrary.com.]

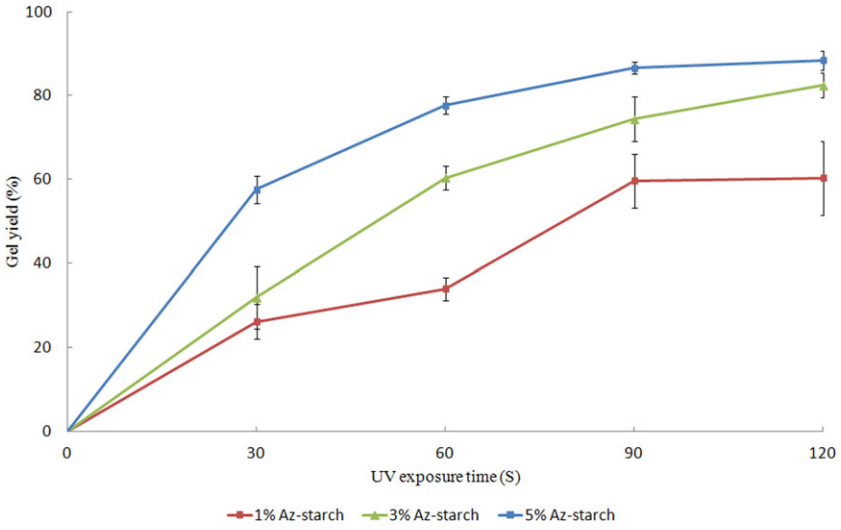


**Figure 6.** The effect of Az-starch concentration and irradiation time on gel yield. Az-starch concentration: 1% (●), 3% (▲) and 5% (■). Each values (mean ± SD, $n = 3$) are represented as the gel yield percentage of the total amount of Az-starch. [Color figure can be viewed in the online issue, which is available at wileyonlinelibrary.com.]

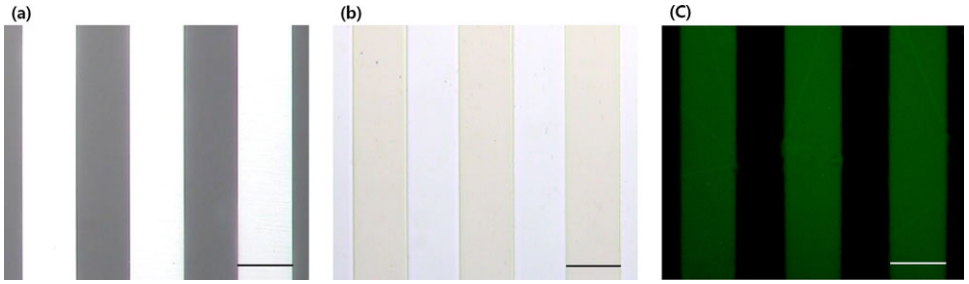


**Figure 7.** Optical micrographs of (a) stripe micropattened plate, (b) Az-starch micropatterned surface and (c) Az-starch micropatterned surface containing FITC-BSA. (Scale bar = 100 $\mu$m).[Color figure can be viewed in the online issue, which is available at wileyonlinelibrary.com.]

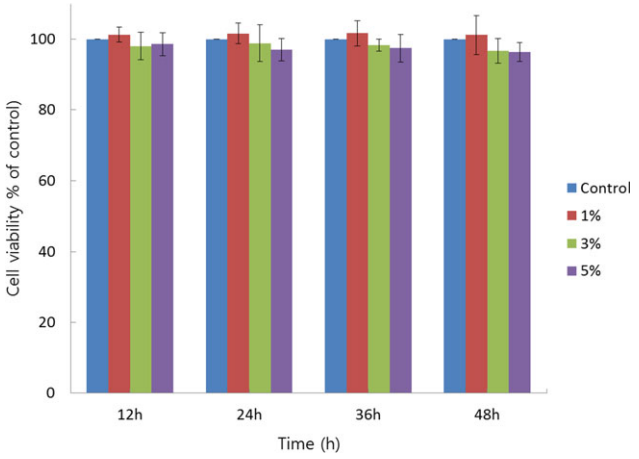


**Figure 8.** Cytotoxicity effect of Az-starch on 3T3-L1 cells. 3T3-L1 cells were treated with various concentrations of Az-starch and cultured for the indicated periods. Cell viability was determined by a WST-8 assay. Untreated cells with Az-starch served as negative controls. Each value (mean ± SD of eight wells) represents cell viability as percentage of corresponding controls. [Color figure can be viewed in the online issue, which is available at wileyonlinelibrary.com.]

azidophenyl groups in Az-starch was determined by comparing the integration of peak intensities attributed to the aromatic protons of Az-starch with methyl protons of carboxymethyl starch. The degree of substitution was found to be 1.86%.

### Photocuring Characteristics

The photocuring characteristics of Az-starch were examined as a function of sample concentration and UV irradiation time (Figure 6). It was observed that longer UV irradiation time or higher Az-starch concentration increased gel yield by increasing crosslinking density and reducing hydrophilicity. Moreover, Az-starch solution with a low concentration gave satisfactory results, transformed to gel in a few seconds of UV irradiation. These results suggest that varying the Az-starch concentration and UV irradiation time could control the release of growth factor immobilized on the sample due to variable crosslinking density.

### Micropattern Immobilization

Photoreactive Az-starch was coated on polystyrene plates, and the coated surface was irradiated with UV light under a stripe micropatterned plate [Figure 7(b)]. The irradiated surface pattern was the inverse of the stripe micropatterned shape. In contrast, nonirradiated Az-starch did not remain on the surface. The micropattern was observed by optical microscopy. It was thought that azido groups exposed to UV irradiation decomposed to $N_2$ and nitrene groups, which are highly reactive radicals. These groups were thought to form intra- and intermolecular covalent bonds with neighboring nitrene groups, as well as with the polystyrene plate [Figure 1(b)].

The properties of the Az-starch-immobilized surface were investigated by contact angle measurement. The contact angle of the Az-starch-immobilized surface (38.9° ± 1.5°) was lower than the Az-starch nonimmobilized surface (84° ± 1.1°). These results suggest that the Az-starch-immobilized surfaces were completely covered via the photo-immobilization method.

The resultant micropattern for aqueous solutions of Az-starch containing FITC-BSA was observed under fluorescence microscopy [Figure 7(c)]. The micropattern on the surfaces was the inverse of that of the stripe micropatterned plate and FITC fluorescence was readily observed. The present results indicate that FITC-BSA was immobilized on the polystyrene plate.

### *In Vitro* Cytotoxicity Test

To evaluate the cytotoxicity of Az-starch under *in vitro* conditions, 3T3-L1 cells were examined in terms of the effect of Az-starch on cell viability using the WST-8 assay with a cell counting kit-8 (CCK-8). Cells treated with 1, 3 and 5 wt % of Az-starch solution were compared with the negative control. In this assay, only cells viable after treatment for predetermined times (12, 24, 36 and 48 h) with Az-starch solution are capable of metabolizing WST-8 efficiently to produce formazan, which is soluble in tissue by the action of mitochondrial dehydrogenase.[25] The data is shown as a cell viability percentage in comparison with the negative control with untreated Az-starch negative controls considered 100% viable. The results indicate that Az-starch solutions in the range of 1–5 wt % are nontoxic

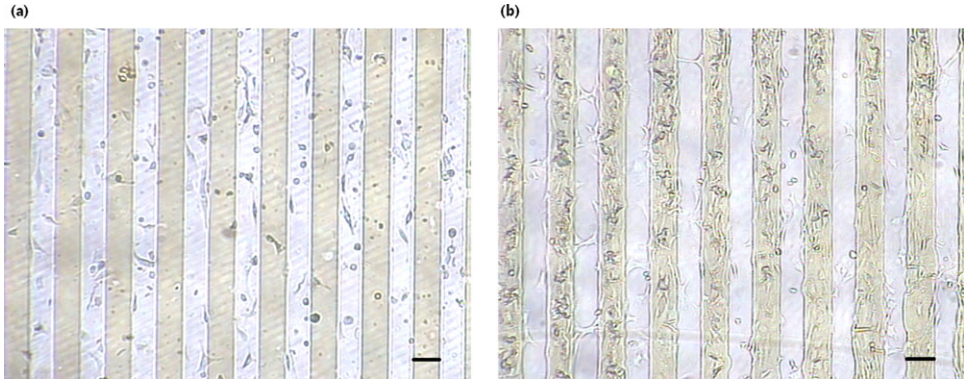


**Figure 9.** Optical micrographs of (a) 3T3-L1 cells on an Az-starch micropatterned surface and (b) 3T3-L1 cells on an Az-starch micropatterned surface containing EGF. (Scale bar = 100 μm).[Color figure can be viewed in the online issue, which is available at wileyonlinelibrary.com.]

Applied Polymer SCIENCE

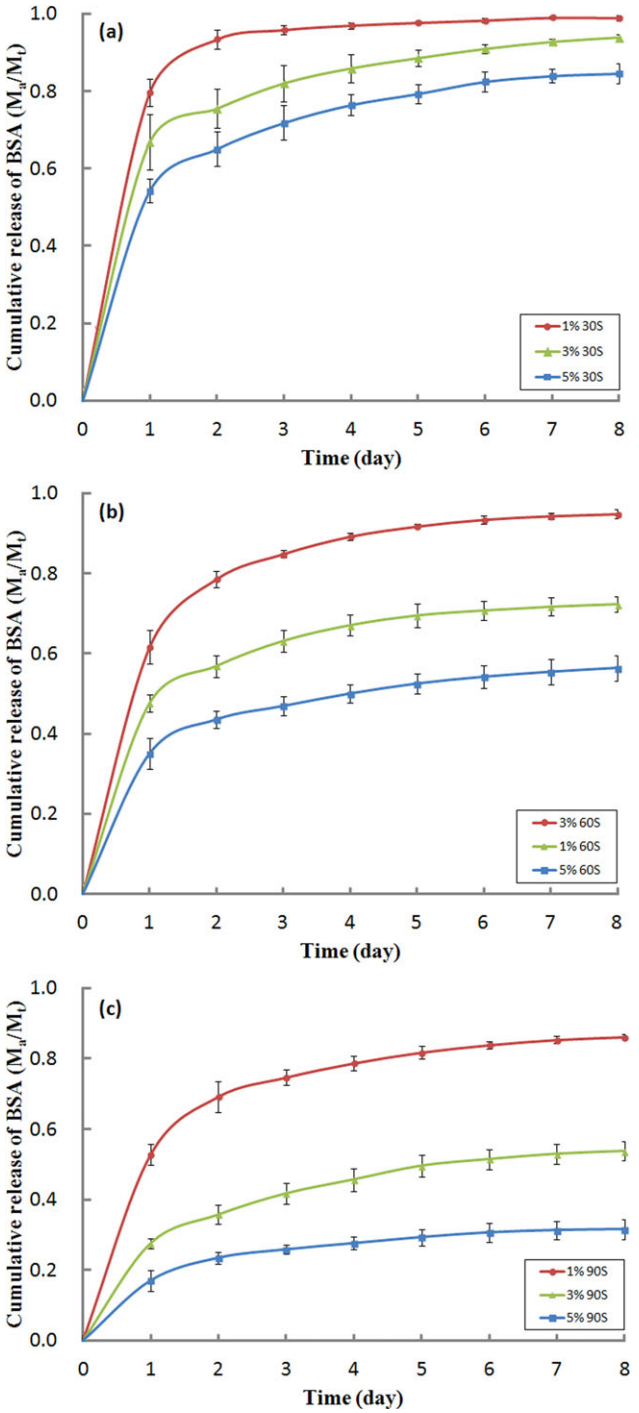


**Figure 10.** *In vitro* fractional release of BSA immobilized in Az-starch with time. Irradiation time: (a) 30 s, (b) 60 s, (c) 90 s and the Az-starch concentration: 1% (●), 3% (▲), and 5% (■). $M_a$ is the amount of released BSA from Az-starch at a given time, $M_t$ is the total amount of loaded BSA in Az-starch at the initial time. Values (mean ± SD, $n = 3$) denote the accumulative release percentage of the amount of total BSA. [Color figure can be viewed in the online issue, which is available at wileyonlinelibrary.com.]

to 3T3-L1 cells (Figure 8). We therefore concluded that the lack of cytotoxicity of Az-starch makes it suitable for applications requiring protein release.

### Cell Culture Studies

The behavior of 3T3-L1 cells after 24 h of culture on the stripe micropatterned surface of immobilized EGF is shown in Figure 9. When the cells were added to the sample plate without EGF immobilization, the cells randomly distributed independent of the immobilized and non-immobilized surface. These cells adhered in a pattern determined by the EGF immobilized and non-immobilized regions. However, on the sample plate with immobilized EGF, most of the cells were observed on the EGF immobilized regions. It was concluded that EGF immobilized on Az-starch surfaces enhanced the adhesion and growth of these adherent cells, although the Az-starch-immobilized surface formed a diffuse hydrophilic layer similar to the conventional property of hydrogel surfaces, which reduce interactions with cells.[26] It is also thought that cell morphology was influenced by surface topography, which was reflected in the cell orientation behaviors due to the stripe dimensions.

### *In Vitro* Protein Release Studies

BSA was used as a model protein and was mixed with sample solution and immobilized by exposure to UV light. Figure 10 shows the accumulative release (%) of the fractional amount of BSA for various immobilized samples prepared with predetermined sample concentrations and UV irradiation times. This figure reveals that the release rates from 1 to 8 days were nearly identical after an initial burst. The accumulative release rate was calculated by dividing the amount of fractional BSA released by the elapsed time and comparing it with the total amount of BSA. According to the results, the release rate and final fractional release were dependent on sample concentration and UV irradiation time. An increase in sample concentration and UV irradiation time clearly decreased the extent of the initial protein burst. The results also suggest that the retention of BSA at the initial burst could effect the immobilized surface wettability, which confers a more sustainable release profile from a hydrophilic sample surface.[27] The release of the blank sample was not affected with the measurement of the released protein amount (data not shown).

### Cell Growth Assay on an EGF-immobilized Surface

The effect of the EGF immobilized Az-starch on cell growth was assessed by measuring formazan absorbance over a 4-day period. Although small amounts of EGF were immobilized in the Az-starch, the number of cells was distinctly higher compared to that of the control containing water-soluble native EGF (Figure 11). Moreover, the cell growth on EGF immobilized Az-starch was approximately proportional to the amount of immobilized EGF on the Az-starch incubated over 96 h. According to the results, there was sufficient interaction between the EGF receptors of the adhered cells and the immobilized EGF to affect mitogenic activity, and the immobilized EGF on the Az-starch inhibited the internalization process that can decrease the continuous effect of EGF on mitogenic activity. These results are regarded that cell growing accelerations are not significantly different from previous reported method which has used chemically modified EGF to photo-immobilize on the

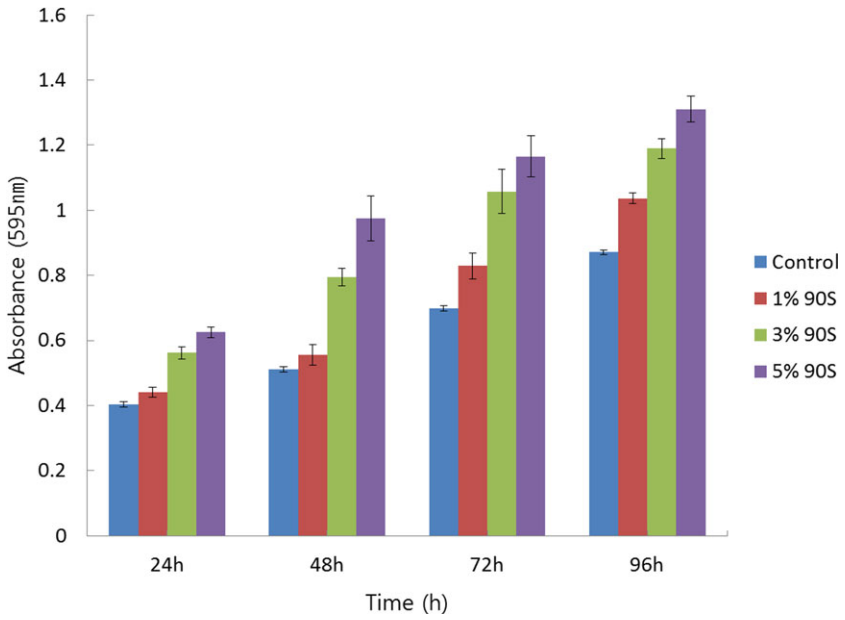


**Figure 11.** Growth of 3T3-L1 fibroblast cells on Az-starch in the presence of various concentrations of photo-immobilized EGF. The cell growth was determined by MTT assay and expressed as the formazan absorbance (mean ± SD of three wells) of 3T3-L1 cells incubated in the polystyrene plate over 4 days. DMEM with 5% (v/v) FBS was supplemented in the control group. [Color figure can be viewed in the online issue, which is available at wileyonlinelibrary.com.]

surface directly.[28] Therefore, it can be concluded that the EGF immobilized on the Az-starch could consistently activate the EGF receptors of fibroblast cells and maintain higher mitogenic activity for an extended period of time.

## CONCLUSIONS

We synthesized a photoreactive Az-starch and demonstrated the photo-immobilization of Az-starch on a polystyrene plate. The polymer-immobilized EGF interacted with fibroblast cells on a patterned plate. The release of protein can be controlled by manipulating Az-starch concentration and irradiation time, which requires a relatively small release burst. The immobilized EGF on the Az-starch was maintained its mitogenic activity which substantially increased the rate of cell turn over, and thereby stimulated the proliferation of 3T3-L1 fibroblast. We thought that there was no significantly difference between immobilizing EGF by Az-starch and chemically modified EGF on surface. Therefore, we considered that Az-starch could be applied as matrix for regulating of cell growth or protein release.

## ACKNOWLEDGMENTS

This research was supported by the Basic Science Research Program through the National Research Foundation of Korea (NRF) funded by the Ministry of Education, Science and Technology (KRF-2011-0009240) and the Chung-Ang University Excellent Student Scholarship in 2012.

## REFERENCES

1. McGeachie, J.; Tenant, M. *Aust. Dent. J.* **1997**, *42*, 375.
2. Carpenter, G.; Cohen, S. *J. Biol. Chem.* **1990**, *265*, 7709.
3. Ito, Y.; Zheng. J.; Liu. S. Q.; Imanishi. Y. *Mater. Sci. Eng. C.* **1994**, *2*, 67.
4. Sharon, J. L.; Puleo. D. A.; *Acta Biomater.* **2008**, *4*, 1016.
5. Papanas, N.; Maltezos, E. *Drug saf.* **2010**, *33*, 455.
6. Vögelin, E.; Jones, N. F.; Huang, J. I.; Brekke, J. H.; Toth, J. M. *Tissue Eng.* **2000**, *6*, 449.
7. Grabarek, Z.; Gergely, J. *Anal. Biochem.* **1990**, *185*, 131.
8. Ito, Y. *Biotechnol. Prog.* **2006**, *22*, 924.
9. Hypolite, C. L.; McLernon, T. L.; Adams, D. N.; Chapman, K. E.; Herbert, C. B.; Huang, C. C.; Distefano, M. D.; Hu, W. S. *Bioconjugate Chem.* **1997**, *8*, 658.
10. Caeole, I.; Gao, H.; Sigrist, H. *Langmuir* **2002**, *18*, 2463.
11. Mizutani, M.; Arnold, S. C.; Matsuda, T. *Biomarcomolecules* **2002**, *3*, 668.
12. Masters, K. S. *Marcomol. Biosci.* **2011**, *11*, 1149.
13. Balmayor, E. R.; Tuzlakoglu, K.; Marques, A. P.; Azevedo, H. S.; Reis, R. L. *J. Mater. Sci. Mater. Med.* **2008**, *19*, 1617.
14. Reis, A. V.; Guiherme, M. R.; Moia, T. A.; Mattoso, L. H. C.; muniz, E. C.; Tambourgi, E. B. *J. Polym. Sci. part A: Polym. Chem.* **2008**, *46*, 2567.
15. Volkert, B.; Loth, F.; Lazik, W.; Engelhardt, J. *Starch/Stärke* **2004**, *56*, 307.
16. Ito, Y. *J. Inorg. Biochem.* **2000**, *79*, 77.
17. Zhang, Y.; Zhu, W.; Wang, B.; Ding, J. *J. Control Release* **2005**, *105*, 260.

18. Goheen, S. M.; Wool, R. P. *J. Appl. Polym. Sci.* **1991**, *42*, 2691.
19. Kacurakova, M.; Wilson, R. H. *Carbohydr. Polym.* **2001**, *44*, 291.
20. Kalutskaya, E. P. *Vysokomol. Soyed.* **1998**, *30*, 867.
21. Fang, J. M.; Fowler, P. A.; Tomkinson. J.; Hill, C. A. S. *Carbohydr. Polym.* **2002**, *47*, 245.
22. van Soeat, J. J. G.; De Wit, D.; Tournois, H.; Vliegenthart, J. F. G. *Starch/Stärke* **1994**, *46*, 453.
23. Capek, P.; Drábik, M.; Turjan, J. *J. Therm. Anal. Calorim.* **2010**, *99*, 667.
24. Jadhav, A. V.; Gulgas, C. G.; Gudmundsdottir, A. D. *Eur. Polym. J.* **2007**, *43*, 2594.
25. Leonard, K.; Ahmmad, B.; Okamura, H.; Kurawaki, J. *Colloids Surf. B: Biointer.* **2011**, *82*, 391.
26. Ito, Y.; Imanishi, Y. *Biomaterials* **1987**, *8*, 464.
27. Han, Z. H.; Ostrikov, K. K.; Tan, C. M.; Tay, B. K.; Peel, S. A. F. *Nanotechnology* **2011**, *22*, 5712
28. Chen, G.; Ito, Y.; Imanishi, Y. *Biochim. Biophys. Acta* **1997**, *1358*, 200.